ELSEVIER

Biophysical Chemistry 124 (2006) 180–191

Biophysical Chemistry

http://www.elsevier.com/locate/biophyschem

Ion solvation and water structure in potassium halide aqueous solutions

Alan K. Soper [a,*], Kristian Weckström [b]

[a] ISIS Facility, Rutherford Appleton Laboratory, Chilton, Didcot, Oxon OX11 0QX, United Kingdom
[b] Turku Centre for Biotechnology, University of Turku Åbo Akademi University, P.O. Box 123, FIN-20521, Turku, Finland

Received 11 December 2005; accepted 12 April 2006
Available online 15 May 2006

Abstract

The structure of water and the nature of ionic hydration is explored in aqueous solutions of potassium fluoride, chloride, bromide and iodide over a range of concentrations up to 4.8 ion pairs per 100 water molecules, using the combined techniques of neutron diffraction with hydrogen isotope substitution. The diffraction data are interpreted using the method of empirical potential structure refinement, which attempts to build a three-dimensional model of the scattering system consistent with the diffraction data. The water structure is strongly perturbed in the first hydration shells of both anion and cation, but is found to be only mildly perturbed outside of this region, with the largest effects occurring with the smallest anion and highest concentrations. For the potassium ion there are strong orientational correlations in the first hydration shell, with the water molecules lying with their dipole moments pointing almost directly away from the cation on average, but with an angular spread of $\sim\pm60°$ which is mildly dependent on the anion type present. For all the anions the water molecules in the first shell are strongly oriented with one O–H vector pointing directly towards the anion on average, with an angular spread of $\sim\pm10°$ for F^-, increasing to $\sim\pm22°$ for I^-. For both anions and cations the second hydration shell is much more disordered than the first, but there is a weak pattern of orientational correlation which becomes more pronounced with the larger anions. There is some evidence that the fluoride ion structures water significantly in its first hydration shell, but not beyond. The findings throw further light on recent findings that the orientational relaxation time for water outside the first shell of dissolved ions is the same as in the bulk liquid.

Keywords: Potassium halides; Aqueous solutions; Neutron diffraction; Hydrogen isotope substitution; Empirical potential modelling; Water structure; Ion hydration; Ion–ion correlations

1. Introduction

There has been a great deal of debate for more than a century on the effect that dissolved ions have on the structure of water. A central theme of that discussion has been the notion that different ions have "structure making" or "structure breaking" effects on water, depending on the ionic size and whether they are cations or anions. Several difficulties emerge in this description however, perhaps the most central being what exactly is meant by structure making and breaking? Naively, we might assume that a structure making ion enhances the tetrahedral network of water, making it more ice-like, while a structure breaking ion has the opposite effect, as happens for example when water is pressurised [1], namely a partially or completely broken tetrahedral network is created. The concept is however difficult to quantify, and even to the present day there is evidence for much confusion over what exactly is meant by the terms. For example, in recent accounts [2,3] of the effect of different ions in affecting the self-assembly of surfactants and hydrophobes, halide anions larger than Cl^- in the Hofmeister series, i.e. Br^- and I^-, are regarded as water structure breakers, while smaller ions such as F^- are regarded as water structure makers. Yet it could equally be argued that a smaller ion, with its much greater local charge density, would be more likely to pull the water away from its hydrogen bonded configuration in the liquid than a larger ion, thus *breaking* the water structure. For example Hribar et al. [3] conclude that "Small ions (kosmotropes) have high charge densities so they cause strong electrostatic ordering of nearby waters, breaking hydrogen bonds." In other words an ion which breaks water hydrogen bonds is regarded as a structure maker.

Data for or against the structure making/breaking concept is generally hard to come by. It has sometimes been invoked indirectly via the solvation entropy [3]. However there is very

* Corresponding author.
E-mail address: a.k.soper@rl.ac.uk (A.K. Soper).

0301-4622/$ - see front matter © 2006 Published by Elsevier B.V.
doi:10.1016/j.bpc.2006.04.009

little direct structural evidence in the form of diffraction data on water structure, even though the nature of ionic hydration has been studied extensively [4]. In the case of amphiphilic or hydrophobic molecules there is a growing body of results indicating that water structure is largely unaffected by the presence of these entities [5 6]. This is in spite of the long-standing view that water should be more ice-like near hydrophobic entities [7]. Even in the case of the large tetramethylammonium ions in water [8], the water structure did not appear to be strongly perturbed.

Recently, femtosecond pulse-probe infra-red spectroscopy on ionic aqueous solutions has thrown valuable new light on the issue of how ions might structure the water around them [9]. The reorientational relaxation time of an excited water molecule is measured both near and far from the ions, and it is concluded that outside the first hydration shell the reorientation time is the same as in bulk water. It is argued that this implies the water structure outside the first shell cannot be strongly restructured compared to the bulk liquid. While this method is also strictly not a probe of structure–the molecule has to be excited to see the effect, and the result is a relaxation time rather than a structure–it is nonetheless a powerful indication that the conventional discussion in terms of structure makers and breakers may have to be revised. The authors surmise that the observed changes in viscosity when small highly charged ions are present arise from the ion retaining its hydration shell as it moves through the liquid, making it a slower diffusing species. In that case there is no need to invoke the solvent restructuring to explain the viscosity. Of course, as is well known [10], ionic mobilities increase with ionic size initially, but with the largest ions, such as Cs^+ and I^-, they decrease again, suggesting that the length of time a water molecule stays in contact with an ion is an important factor in determining its mobility.

Since the earlier neutron diffraction work on amphiphiles and tetramethylammonium ions in solution [5,8], there have been significant developments in our ability to interpret diffraction data. In particular it is now possible to perform a computer simulation of the data and obtain both a 3-dimensional model of system under investigation as well as estimates for the complete set of site–site radial distribution functions, which are consistent with the diffraction data [11,12]. Once established, the model can be further explored to look for other structural quantities, such as the orientational distribution of water around the ions, and water–water–water angle distributions [13,14], which are a sensitive indicator of the degree of tetrahedral order in water. It was therefore timely to revisit the old problem of ions in water, and attempt to address some of these questions about the degree to which ions can affect water structure. The present experiment was motivated by a desire to understand why anions in particular appear to have a marked influence on apparent molal enthalpies of mixing of surfactants with water [15].

2. Experiment

The data were measured on the Small Angle Neutron Diffractometer for Amorphous and Liquid Samples (SANDALS) at the ISIS pulsed neutron source (UK). This instrument concentrates its neutron detectors at scattering angles below ~40°, which helps to reduce, but not eliminate, the effects of nuclear recoil when scattering neutrons from materials containing hydrogen. The potassium halide salt solutions were chosen for this study partly because of the ability to make solutions for all four potassium halide salts with the same concentrations, namely KF, KCl, KBr and KI, and partly because potassium is regarded as being rather neutral in its effect on water structure [3]. Hence we can in principle study the effects of the anions directly. The salt/water mole ratios chosen for this study were 1.2:100, 2.4:100 and 4.8:100, giving a total of 12 solutions. In addition for each solution three samples were prepared, namely a solution in heavy water, D_2O, a solution in light water, H_2O, and a solution in a 50:50 mole ratio mixture of D_2O and H_2O, here labelled as HDO. High purity samples of the various salts were obtained from Sigma-Aldrich and used without further processing. The use of isotope contrast with neutron diffraction is a powerful probe of local structure in such solutions, because of the large contrast in neutron scattering length between H (−3.74 fm) and D (6.77 fm), which greatly assists in delineating the different site–site distributions that are needed to describe these solutions. The samples are contained in specially made TiZr alloy cans which produce negligible coherent scattering due to the cancellation of the Ti and Zr scattering lengths [16], while at the same time being quite corrosion resistant.

The diffraction data are analysed to differential cross-section detector by detector using a program called “Gudrun”, which is an up-to-date version of the previous ATLAS routines [17]. Standard corrections for attenuation, multiple scattering and container scattering are performed, and the data are placed on absolute scale of differential cross section by calibrating the detectors against a known vanadium sample. A further correction then has to be made for single atom scattering, which for protons can have a pronounced dependence on the wave vector transfer, Q. This has been described previously [18]. After removing the single atom scattering the result is the interference or distinct differential scattering cross-section,

$$F_{\mathrm{d}}(Q) = \sum_{\alpha,\beta\geq\alpha} (2-\delta_{\alpha\beta}) c_\alpha c_\beta b_\alpha b_\beta H_{\alpha\beta}(Q) \qquad (1)$$

where the Kronecker $\delta_{\alpha\beta}$ is to avoid double counting atom pairs of the same type, c_α and b_α are the atomic fraction and neutron scattering length respectively of component α, and the partial

Table 1
Atomic fractions used in the present study of potassium halide aqueous solutions

	Molar ratio 1.2:100	Molar ratio 2.4:100	Molar ratio 4.8:100
c_{Ow}	0.3307	0.3281	0.3230
c_{Hw}	0.6614	0.6562	0.6460
c_{K}	0.0040	0.0079	0.0155
c_{X}	0.0040	0.0079	0.0155

The water oxygen and hydrogen atoms are referred to as Ow and Hw respectively. X represents the relevant halide ion.

structure factor, $H_{\alpha\beta}(Q)$, is related to the corresponding site–site radial distribution function, $g_{\alpha\beta}(r)$ via Fourier Transform,

$$H_{\alpha\beta} = 4\pi\rho \int r^2 \left(g_{\alpha\beta}(r)-1\right) \frac{\sin Qr}{Qr} \mathrm{d}r, \quad (2)$$

with ρ as the total atomic number density. In the present instance, densities were taken from the Handbook of Chemistry and Physics [19]. Based on the neutron scattering lengths and atomic fractions of the 12 samples, the neutron weightings in Eq. (1) can be evaluated. The relevant atomic fractions are given in Table 1.

3. Empirical potential structure refinement

The traditional approach to understanding diffraction data from multicomponent systems is to combine the data from different isotope contrasts, and including data from X-ray diffraction if present, and attempt to extract the individual site–site partial structure factors and radial distribution functions by inverting the scattering weights matrix [20]. In the case where incomplete isotope substitutions are available, then composite partial structure factors can be extracted [18]. With empirical potential structure refinement (EPSR) [12] however it is possible to take a more holistic approach in which one combines several pieces of information together with the diffraction data and attempts to generate a 3-dimensional distribution of atoms and molecules which is as consistent as possible with the known facts. This is therefore an extension of the popular Reverse Monte Carlo method [21], which in general makes hard-sphere assumptions on atomic overlap and uses square well potentials to define molecules [22]. In EPSR on the other hand, molecules are defined by harmonic forces, which give a more realistic spread in the intramolecular distribution functions, and intermolecular forces can include repulsive core, dispersion and Coulomb forces, as well as the empirical potential derived from the diffraction data. Hence the aim in EPSR is not to find the most disordered distribution which is consistent with the diffraction data [21], but a distribution which is consistent with both the diffraction data and other assumed quantities, such as the molecular structure, the ionic charges, the effective charges on the water molecule, and the hydrogen bonding between water molecules. None of this guarantees the outcome is correct, particularly as there is the possibility that systematic error derived from incomplete subtraction of the single atom scattering might get transferred into the final functions, but it does at least satisfy the consistency criteria, which cannot be said of methods which analyse the diffraction data directly to radial distribution functions [20].

Table 2
Lennard-Jones and charge parameters used in the simulation of potassium halide aqueous solutions

α	ε_α [kJ/mol]	σ_α [Å]	q_α [e]
Ow	0.6500	3.166	−0.8476
Hw	0.0000	0.000	+0.4238
K	0.5144	2.940	+1
F^-	0.5660	3.080	−1
Cl^-	0.5660	4.191	−1
Br^-	0.5660	4.538	−1
I^-	0.5660	5.094	−1

Table 3
Cubic box dimensions and number densities used in the simulation of potassium halide aqueous solutions

		No. of cations	No. of anions	Box dimension [Å]	Atomic number density [atoms/Å^3]
Mole ratio 1.2:100	KF	12	12	31.1342	0.10020
	KCl	12	12	31.2347	0.09915
	KBr	12	12	31.2912	0.09870
	KI	12	12	31.3623	0.09803
Mole ratio 2.4:100	KF	24	24	31.1956	0.10040
	KCl	24	24	31.4482	0.09800
	KBr	24	24	31.5343	0.09720
	KI	24	24	31.6838	0.09583
Mole ratio 4.8:100	KF	48	48	31.3794	0.10020
	KCl	48	48	31.8526	0.09580
	KBr	48	48	32.0331	0.09419
	KI	48	48	32.2666	0.09216

There are 1000 water molecules in each box, and the number of anions and cations in each box is given in the table as a function of mole ratio.

In EPSR a reference potential is set up which is used to define and equilibrate the starting configuration of molecules. This reference potential is of the form Lennard-Jones plus Coulomb:

$$U_{\alpha\beta}(r) = 4\varepsilon_{\alpha\beta}\left[\left(\frac{\sigma_{\alpha\beta}}{r}\right)^{12} - \left(\frac{\sigma_{\alpha\beta}}{r}\right)^{6}\right] + \frac{q_\alpha q_\beta}{4\pi\varepsilon_0 r} \quad (3)$$

The Coulomb potential is truncated by the method of Hummer et al. [23], using a cut-off radius of 12 Å. The Lennard-Jones potential is truncated smoothly at the same distance. In the present case the water molecule is represented by an OH bond of length 0.98 Å and an HH bond of length 1.56 Å, with r.m.s. deviations in these values of ~0.073 Å and 0.108 Å, respectively. The Lennard-Jones and effective charge values are set to those of the SPC/E model of water [24]. For the ions, the Lennard-Jones values seem to vary slightly from source to source [10,25], so the values adopted here have been chosen to reproduce approximately the known water–ion distances [4]. Table 2 gives a list of all the assumed Lennard-Jones and charge values. The cross terms are obtained by the Lorentz-Berthelot mixing rules: $\sigma_{\alpha\beta} = \frac{1}{2}(\sigma_\alpha + \sigma_\beta)$, and $\varepsilon_{\alpha\beta} = \sqrt{\varepsilon_\alpha \varepsilon_\beta}$.

Boxes of atoms were made up consisting of 1000 water molecules and the relevant number of cation–anion pairs, namely 12, 24 and 48 for the respective mole ratios. Table 3 lists the box sizes and number densities that have been used. After an initial equilibration period with the reference potential on its own, the empirical potential, derived from the difference between the measured and simulated interference differential cross-section [11], is added to the reference potential as a perturbation. The perturbed potential becomes the new potential in the simulation, and this process repeats itself a large number of times until the simulated diffraction cross-sections match as close as possible the measured data. After that the simulation can be run indefinitely, accumulating suitable structural quantities.

In the present work we will concentrate on the site–site radial distribution functions that are obtained from these simulated boxes of atoms, the ion water coordination numbers (hydration

numbers) and the triple atom angle distribution functions [13,14], $P(\theta)$, which is sensitive to the degree of orientational correlation between an ion and its neighbouring water molecules, and the extent of hydrogen bonded network in water. These angle distribution functions are defined so that if $P(\theta)=c$ for all θ, where c is a constant, then the corresponding vector is randomly oriented with respect to the origin. Hence to calculate the angular average of some function $a(\theta)$ in the angle range θ_1 to θ_2 we need to evaluate the integral

$$\langle a(\theta)\rangle_{\theta_2-\theta_1} = \frac{\int_{\theta_1}^{\theta_2} a(\theta)P(\theta)\sin\theta \mathrm{d}\theta}{\int_{\theta_1}^{\theta_2} P(\theta)\sin\theta \mathrm{d}\theta}. \quad (4)$$

It has proved quite difficult to constrain the configurational energy and pressure in EPSR. Because the potential is being continuously adjusted depending on how close the simulation fits the data, the energy and pressure are found to fluctuate quite widely, even after a satisfactory fit to the data is found. Such large fluctuations do not occur in simulations where the interaction potential is held fixed throughout the simulation. Presumably this indicates that although the structure couples closely to the details of the local interaction potential, it is rather insensitive to the overall energy, which is an integral over a wide distance range. Hence small long range deviations in the potential may have negligible effect on the structure at short range, but can have a big impact on the overall configurational energy in a simulation where the number of molecules is held fixed in a box of specified size. Hence the failure to constrain both energy and pressure, particularly pressure, to reasonable values indicates there may be a limitation in the method which has yet to be understood. The configurational energies are invariably negative as expected, but the variability of both pressure and energy makes the reporting of their values unreliable.

4. Results

Fig. 1a gives an example of the simulated differential cross sections that are obtained in this work for the KCl data at a mole ratio 2.4:100. Also shown is the difference between data and simulation. It will be noted that although there are some discrepancies at small Q, which almost certainly arise from inadequacies in subtracting the single atom scattering in this Q range, the overall Q-dependence of the difference is of low frequency, and would therefore correspond to unphysical features in r-space. Since systematic errors arising from the single atom scattering subtraction are additive rather than multiplicative, the shape of these difference functions indicates that the simulation has probably captured most if not all of the genuine structural information in the diffraction data. Fig. 1b shows the same data, this time in r-space. Again it is seen that the simulation has captured the main features of the data, and it is not clear whether the residual discrepancies are due to a failure of the EPSR method itself, or from residual systematic effects that are almost certainly present in the data. Fits to all the other datasets are all of equivalent quality and are therefore not shown here.

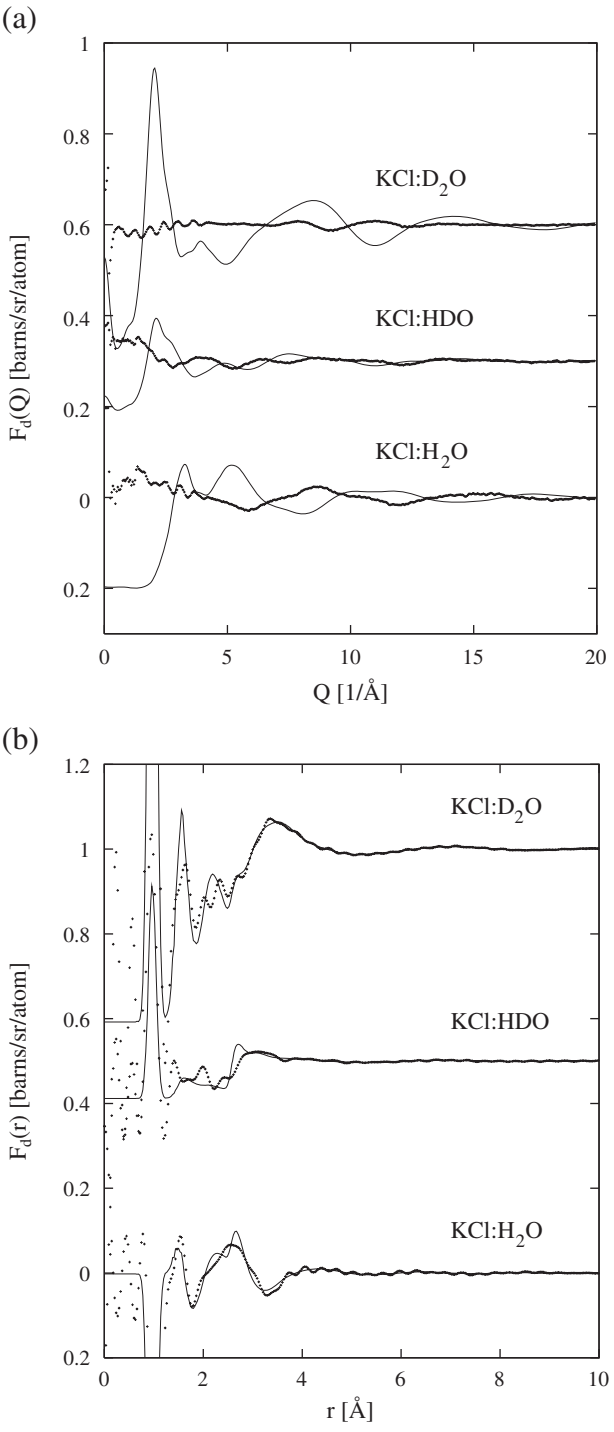

Fig. 1. (a) Interference differential cross-sections for a solution of KCl in water at a mole ratio of 2.4:100 (dots) for different mixtures of heavy and light water. The solid line shows the EPSR fit to these data. (b) Same data as (a) but now in r-space. The $F(r)$ data were obtained by numerical Fourier transform of the diffraction data shown in (a).

4.1. Water structure in solution

Figs. 2 and 3 show the water–water radial distribution functions (rdfs) for the two salts at the extremes of the halide range, namely KF and KI, comparing them with the case of pure water. It is clear that as a general rule these rdfs do not change

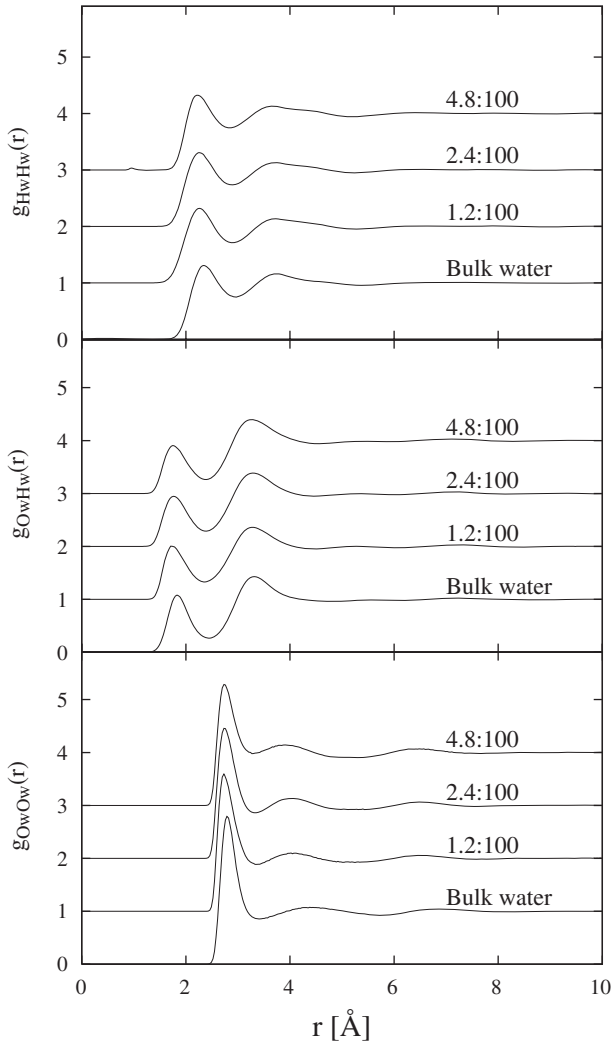

Fig. 2. Water–water radial distribution functions (OwOw, bottom, OwHw, middle, HwHw, top) for ionic solutions of KF as a function of concentration, and compared to the same functions in pure water (bottom curve of each figure).

radically compared to pure water. The main difference is that the second peak in $g_{OwOw}(r)$ at ~4.4 Å in pure water tends to move towards ~4.0 Å in the solutions, the effect being most pronounced at the highest concentration and with the largest anion. This is analogous to the pressure effect that was observed in other ionic solutions, where the changes in the diffraction pattern were shown to be equivalent to what happens when pure water is pressurised [26]. There is some small variability in the position of the second peak in $g_{OwOw}(r)$ as a function of concentration, and it is not clear at this point whether these are real or are possibly artefacts caused by slight variations in the driving force provided by the data. Changes in the OwHw and HwHw functions are more subtle and hard to categorise at these concentrations. Note however that these plots do not distinguish between water near the ions and water away from the ions.

4.2. Cation–water correlations

Fig. 4 shows the potassium–water rdfs, KOw and KHw for all the solutions at a molar ratio of 2.4:100. The same functions at the other concentrations look closely similar. One sees immediately that there are strong local correlations around the potassium ion, with a pronounced hydration shell near 2.7 Å and with the water hydrogen atoms further away on average than the water oxygen atoms. There is a second hydration shell clearly visible with a peak near 4.7 Å, and this becomes slightly more pronounced with the increasing size of the anion. Again one sees that the Hw atoms in this second shell tends to be slightly further away than the Ow, implying there are weak orientational correlations in this second shell as well. To highlight these orientations, we show in Fig. 5(a) the definition of the angle between a cation and the water molecule dipole moment vector, and in Fig. 6 the dipole moment angle distribution, $P(\theta)$, for the first and second shells around potassium. The first or second shell water molecules are determined by their distance from the ion and the position of the first and second minima in the corresponding ion-Ow radial distribution function, Table 4. The first shell distribution shows a strong peak near 180°, corresponding to the water dipole moment pointing directly away from the ion. Table 5 summarises the deviation of the

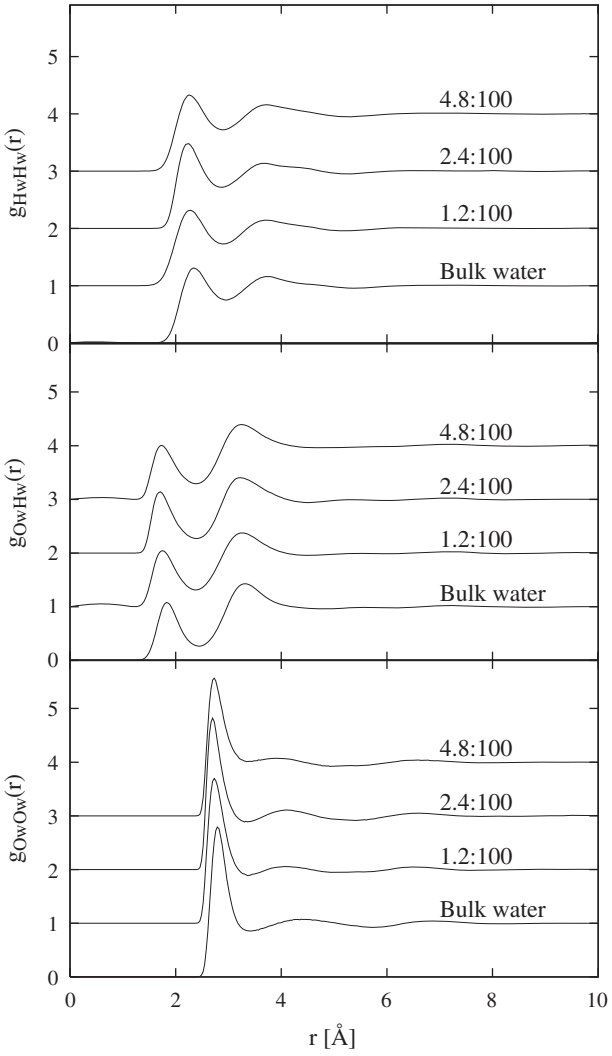

Fig. 3. Water–water radial distribution functions (OwOw, bottom, OwHw, middle, HwHw, top) for ionic solutions of KI as a function of concentration, and compared to the same functions in pure water (bottom curve of each figure).

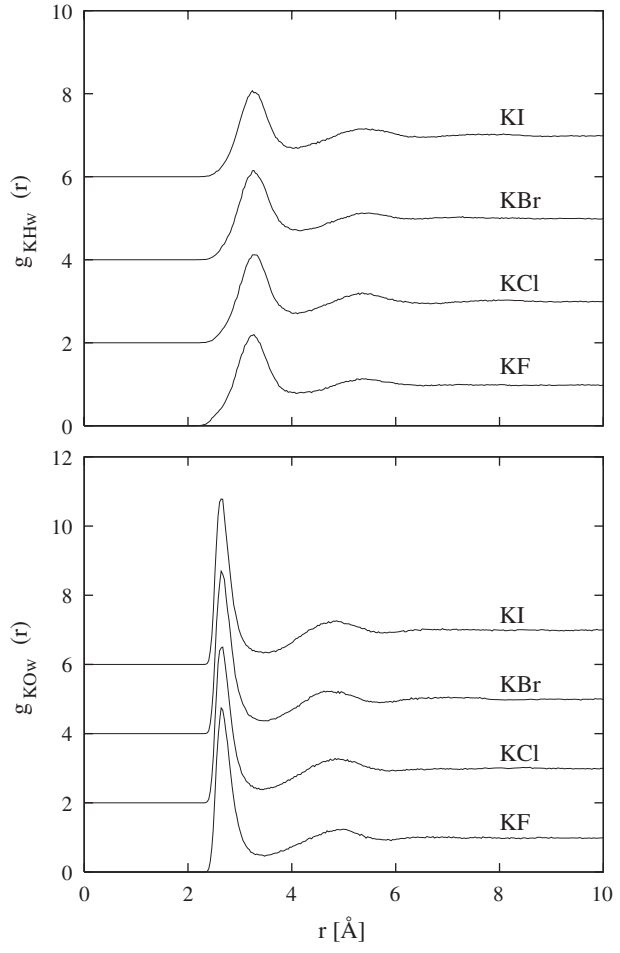

Fig. 4. Potassium ion–water (KOw, bottom, KHw, top) radial distribution functions for K-halide ionic solutions at a molar ratio of 2.4:100.

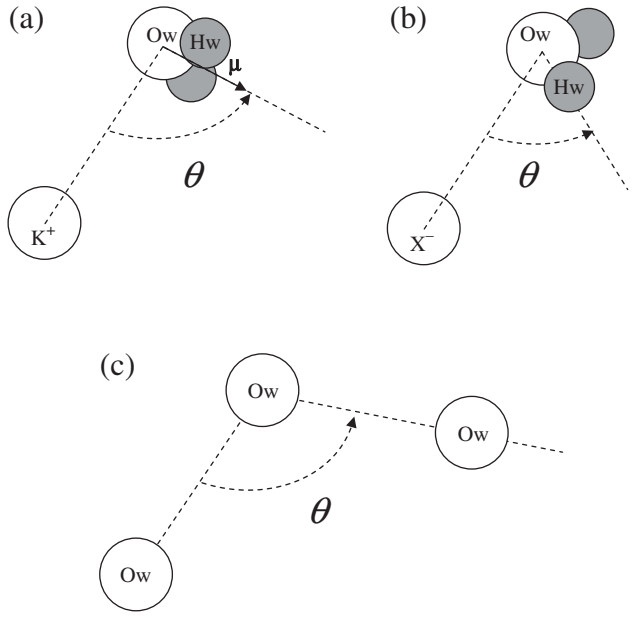

Fig. 5. (a) Definition of the included angle, θ, between a cation and the water molecule dipole moment vector, μ. (b) Definition of the included angle, θ, between an anion and the OH vector on a neighbouring water molecule. (c) Definition of the included angle, θ, between three neighbouring water molecules.

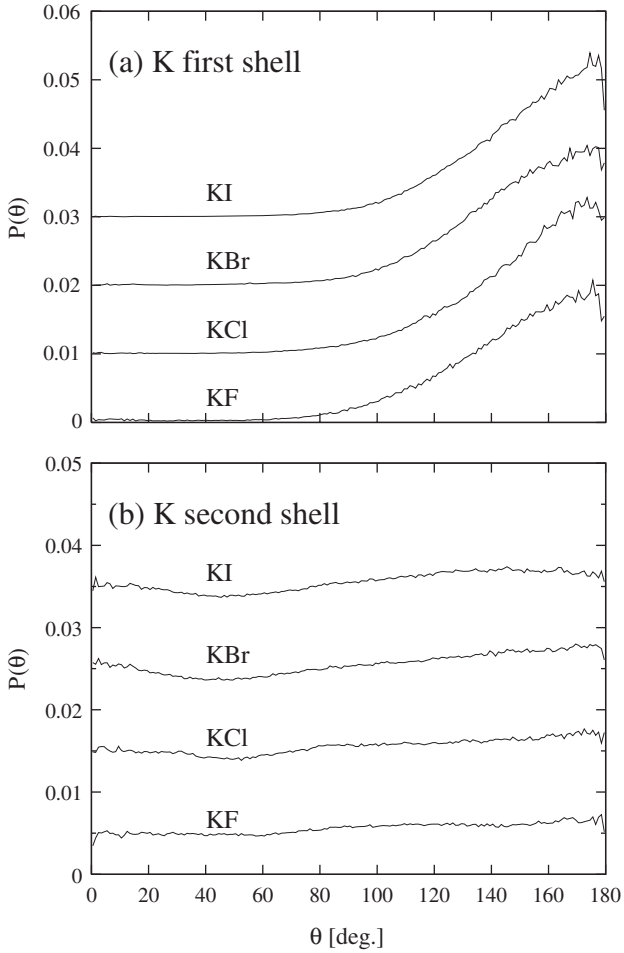

Fig. 6. Potassium ion–water dipole moment angle distributions for K-halide ionic solutions at a molar ratio 2.4:100. The angle plotted is defined in Fig. 5(a).

average angle found for this dipole moment vector from the angle at the peak of the distribution, 180°. It is clear that although this distribution is sharply peaked, it also has quite a broad distribution up to about 80° from the peak, indicating that the cation is binding to the water molecule lone-pair electrons on the average, rather than this being a simple dipolar ordering. The second shell is much more disordered. Nonetheless there are angular correlations in this shell as well, with a broad peak near

Table 4
Distances used to define first and second coordination shells of cations and anions in K-halides aqueous solutions

	Positions [Å]			
	1st peak	1st minimum	2nd peak	2nd minimum
K	2.65	3.45	4.85	6.00
F	2.54	3.27	4.49	5.54
Cl	3.14	3.77	4.99	6.19
Br	3.32	3.90	5.10	6.20
I	3.63	4.10[a]	–	5.90

The distances are taken from the relevant ion–Ow radial distribution function obtained at a molar ratio of 2.4:100. The concentration dependence of these distances is weak. Note that these distances are not well constrained by the present diffraction data, but are consistent with them.

[a] This is an approximate as there is no distinct 1st minimum for this function (see Fig. 7).

Table 5
Average deviation of the angle of the water molecule dipole moment vector about potassium from its most probable value (180°) in the first hydration shell of the potassium ion for aqueous solutions of KF, KCl, KBr and KI all at a molar ratio of 2.4:100

	Potassium ($180-\langle\theta\rangle_{0-180}$) [°]	Anion ($\langle\theta\rangle_{0-60}-0$) [°]
KF	50.4	10.3
KCl	44.8	16.3
KBr	46.2	19.0
KI	48.9	21.6

Also given is the deviation of the average angle between the anion and the OH vector from its most probable value (0°) in the anion first hydration shell. For the anions the average angle has been calculated in the angular range 0–60° to avoid including the second OH vector on the same water molecule.

180°. For the larger anions there is also some evidence for second shell water molecules to have their dipole moment vectors pointing directly towards the cation, presumably hydrogen bonded to the first shell water molecules.

4.3. Anion–water correlations

The anion–water radial distribution functions are shown in Fig. 7. Here we see the reverse of the cation–water distributions, namely one hydrogen is much closer to the anion than the corresponding oxygen atom. The corresponding angular distributions are shown in Fig. 8, using the angle definition given in Fig. 5(b). Now we see that in the first shell the water molecule is strongly directed with the OH vector pointing directly towards the anion in every case. Obviously this interaction is stronger for the smaller anions, but it exists even in the case of the iodine ion, i.e. there is no sign of the dipole ordering that has been speculated about elsewhere. Table 5 shows the average OH vector angle deviates from 0° by as little as 10° for fluorine, increasing up to ~20° for iodine. There is also no sign of a bimodal distribution in any of these functions as some sources have suggested.

Fig. 8 also shows the second shell angular correlations. Here there is clear evidence for a second shell orientational structure, particularly with the iodide counterion, where a broad peak at about 20° with the fluoride ion moves to about 50° with the iodide ion. Presumably this second shell structure arises from hydrogen bonding between the first and second shell and the movement is related to the increased width of the main peak in the first shell orientation with increasing anion size. Hence there is evidence here for a second shell around the halide anion, and that it consists of partly polarised local water structure.

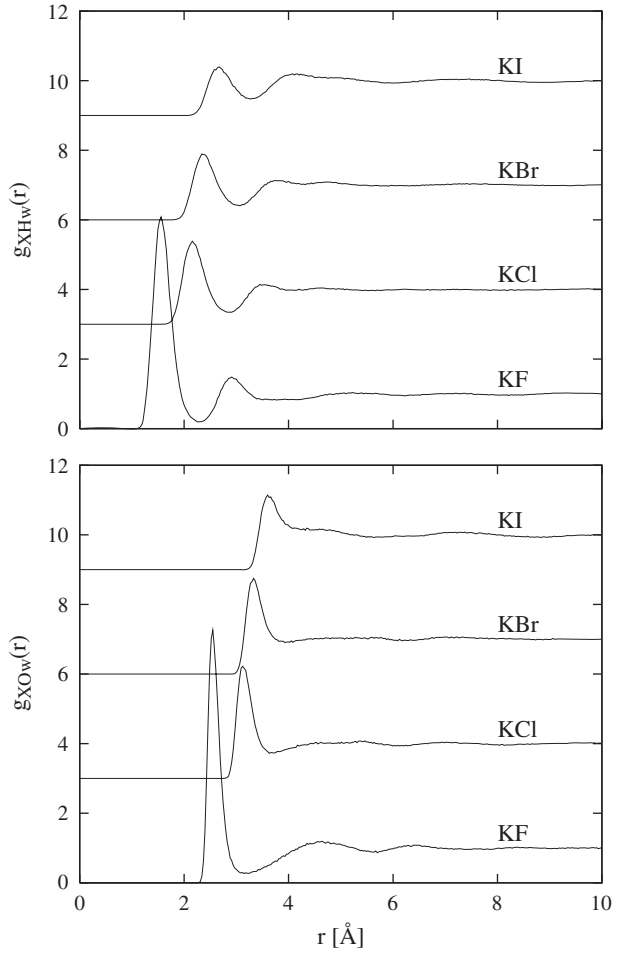

Fig. 7. Halide ion–water (KOw, bottom, KHw, top) radial distribution functions for K-halide ionic solutions at a molar ratio of 2.4:100.

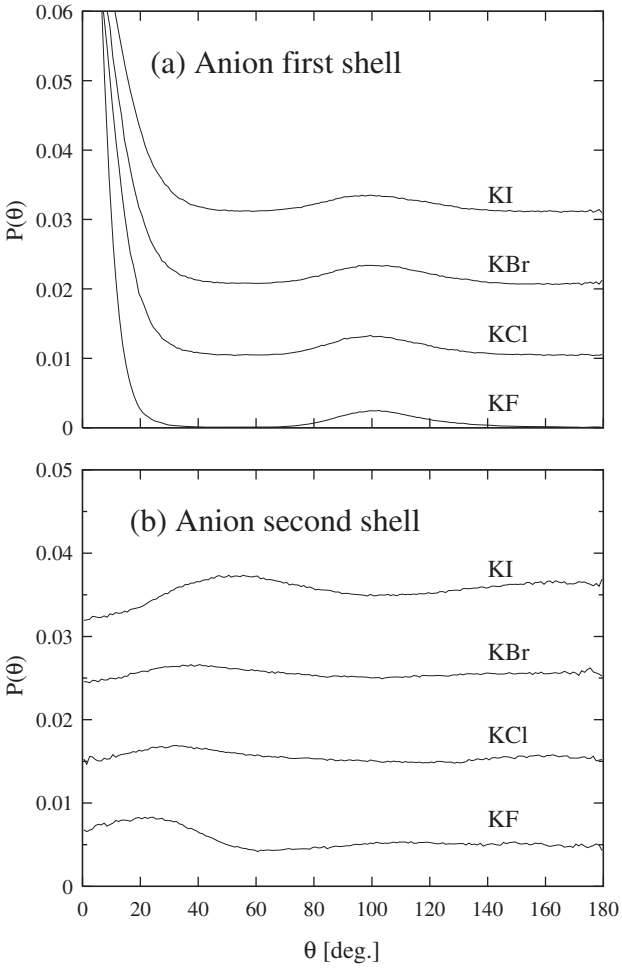

Fig. 8. Halide ion–water OH vector angle distributions for K-halide ionic solutions at a molar ratio 2.4:100. The angle plotted is defined in Fig. 5(b).

4.4. Ion hydration numbers

Table 6 gives a summary the relevant first shell coordination numbers. These coordination numbers are obtained by integrating the relevant site rdf. Thus $N_{\alpha\beta} = 4\pi\rho_\beta \int_{R_1}^{R_2} r^2 g_{\alpha\beta}(r)\mathrm{d}r$ is the number of type β atoms around a central type α atom in the distance range R_1 to R_2.

For the potassium ions we find the ion hydration number is around 6 water molecules and is fairly stable as a function of concentration, with possibly a slight decrease with increasing salt concentration. What is perhaps more surprising is that the anion hydration number, as determined from the anion Hw rdf, is also fairly stable around 5.5–6 water molecules for all the anions, in spite of the steady increase in the distance of the first hydration shell from the ion as we go down the halide series. One might have expected, given this distance increase, that the number of hydrating water molecules would increase with ion size, but apparently not. What seems to happen instead is that there is a pronounced second shell with the fluoride ion, but this starts to overlap increasingly with the first shell for the larger anions, Fig. 7. We note that the number of water hydrogen atoms in the first hydration shell is always smaller than the number of oxygen atoms, indicating there is a fraction of the first hydration shell water molecules that do not bond to the anion. We also note that the hydration number tends to decrease with increasing solute concentration in a much more marked manner than is observed with potassium. Finally it is worth pointing out that the hydration number for chloride found here is very close to values found independently when the hydration shell is measured directly by isotope substitution on the chloride ion [4,27]. This gives at least some confidence that the structure found here by computer simulation of the diffraction data is consistent with independent measurements. Equally the potassium coordination numbers are closely consistent with recent estimates based on ab initio molecular dynamics [28].

Table 6
First shell ion–water coordination numbers for K-halide aqueous solutions

	Coordination number		
KF Molar ratio	N_{KOw} (3.45 Å)	N_{FOw} (3.27 Å)	N_{FHw} (2.28 Å)
1.2:100	6.4	6.9	6.7
2.4:100	6.2	6.0	5.7
4.8:100	5.8	5.2	5.0
KCl Molar ratio	N_{KOw} (3.45 Å)	N_{ClOw} (3.78 Å)	N_{ClHw} (2.88 Å)
1.2:100	6.2	7.1	6.4
2.4:100	5.5	6.2	5.4
4.8:100	5.6	6.4	5.6
KBr Molar ratio	N_{KOw} (3.45 Å)	N_{BrOw} (3.90 Å)	N_{BrHw} (3.03 Å)
1.2:100	5.9	6.7	5.9
2.4:100	5.6	6.4	5.5
4.8:100	5.5	6.4	5.4
KI Molar ratio	N_{KOw} (3.45 Å)	N_{IOw} (4.11 Å)	N_{IHw} (3.27 Å)
1.2:100	6.0	6.7[a]	5.8
2.4:100	5.5	6.6[a]	5.3
4.8:100	5.9	7.1[a]	4.7

The maximum integration range for each number is given in parentheses, and the relevant radial distribution functions are KOw for potassium and XOw and XHw for the halide ion, where X is either F, Cl, Br, or I. The uncertainty on these numbers is believed to be about ±5%.

[a] This value is uncertain due to the lack of a clear minimum after the first peak.

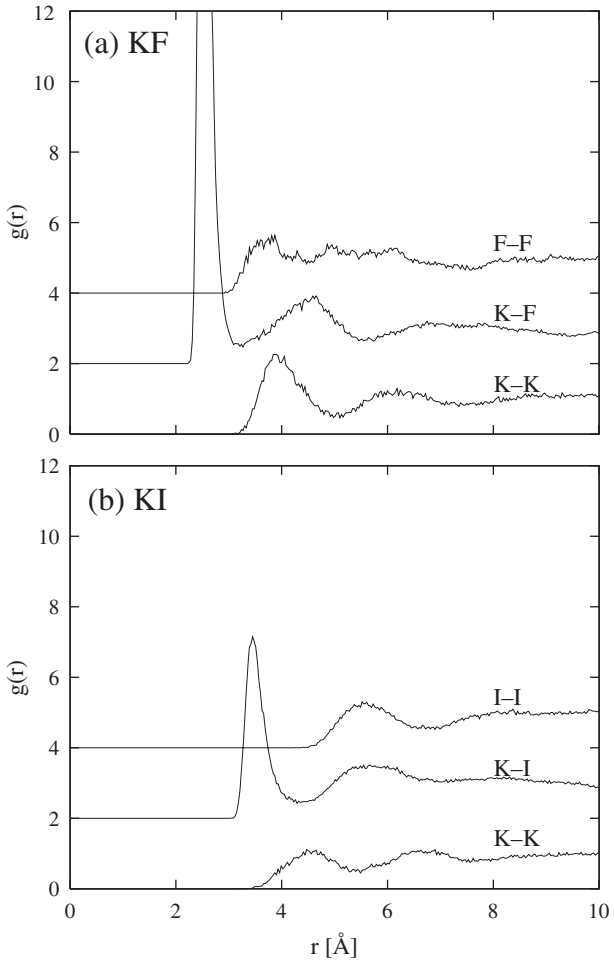

Fig. 9. Ion–ion radial distribution functions for KF (a) and KI (b) ionic aqueous solutions at a mole ratio 2.4:100.

4.5. Ion–ion correlations

The question of how ions correlate in aqueous solutions is the subject of much debate, because there is currently no satisfactory probe of these correlations, except perhaps in some very concentrated solutions of nickel where there is sufficient diffraction contrast for nickel isotope substitution [29], or where isomorphic substitution can be performed [30]. In the present experiments the sensitivity of the data to these correlations is negligible compared to the dominant water–water and water–ion correlations, so any information on ion–ion contacts is derived purely from the computer simulation, and is therefore speculative at best. Nonetheless it is shown here briefly for completeness.

Fig. 9 shows two examples of the ion–ion rdfs for the most concentrated KF and KI solutions. Table 7 lists the K-halide ion contact coordination numbers. It is clear that at all the concentrations studied both ion contact pairs and solvent

Table 7
Potassium-halide ion coordination numbers as a function of concentration

	Coordination number
KF Mole ratio	N_{KF} (3.24 Å)
1.2:100	0.1
2.4:100	0.4
4.8:100	0.9
KCl Mole ratio	N_{KCl} (3.87 Å)
1.2:100	0.1
2.4:100	0.6
4.8:100	0.7
KBr Mole ratio	N_{KBr} (4.14 Å)
1.2:100	0.4
2.4:100	0.7
4.8:100	0.8
KI Mole ratio	N_{KI} (4.41 Å)
1.2:100	0.3
2.4:100	0.7
4.8:100	0.6

The maximum integration range is shown in parenthesis.

separated ion pairs occur. The number of cation–anion contacts increases rapidly with concentration above a mole ratio of 1.2:100, but saturates at around 0.6–0.9 above a mole ratio of 2.4:100. The marked movement of the anion–anion first peak with anion size is only weakly matched by a corresponding movement of the cation–cation first peak, indicating that the charge ordering typical of a molten salt [31] does not occur in these systems. Based on these results it appears that the hydration shell of one ion in these solutions is likely to be shared with up to one counter-ion of the opposite charge, particularly at the higher salt concentrations. Note however that with the exception of the fluoride solutions, the K–Ow first peak is inside the K–anion first peak, while the anion–Ow first peak is about the same distance as the K–anion peak for Cl, Br and I. Hence the K ion will always have its hydration waters in closer proximity than the anions for these three solutions, while the anions can also be carrying up to one counter-ion in their first shells. Obviously the smaller the cation, then the less able is the anion to penetrate the cation first hydration shell. This information is not widely appreciated when discussing the different cation and anion properties in solution.

5. Discussion

By now it will hopefully be apparent that the approach being adopted here to interpret the neutron diffraction data on aqueous solutions is somewhat different from the traditional interpretation of these data based on radial distribution functions derived directly from the data alone [27]. Instead a three-dimensional model is built by computer simulation which uses the diffraction data as a constraint, but which also builds other constraints into the problem, such as the molecular geometry (via the harmonic potential) and the constraints on atomic overlap (via the Lennard-Jones parameters). If it were left at that then there is no question, as shown by several workers [22,32], that a range of structural solutions would be possible all consistent with the diffraction data, but which would likely contain physical absurdities. In other words on their own the diffraction data are not necessarily sufficiently sensitive to the ion–water and ion–ion correlations to be able to constrain these quantities adequately, or even the water structure if only the heavy water diffraction data are available [22].

The distinguishing aspect here is that we have included Coulomb charges on the ions, and effective charges on the water molecule to simulate the effect of hydrogen bonding between water molecules, and between ions and water. These charges greatly limit the region of structural phase space that can be explored by the model. Using EPSR to interpret the data still does not guarantee the results are correct, but it does ensure they are at least consistent with what we think we know about the system before we start, and with the diffraction data. The results are also not necessarily consistent with the configurational energies of the systems, where these are known, and the pressures of the systems, but these quantities are often insensitive to the details of the structure. If a way could be found to constrain these quantities alongside the diffraction

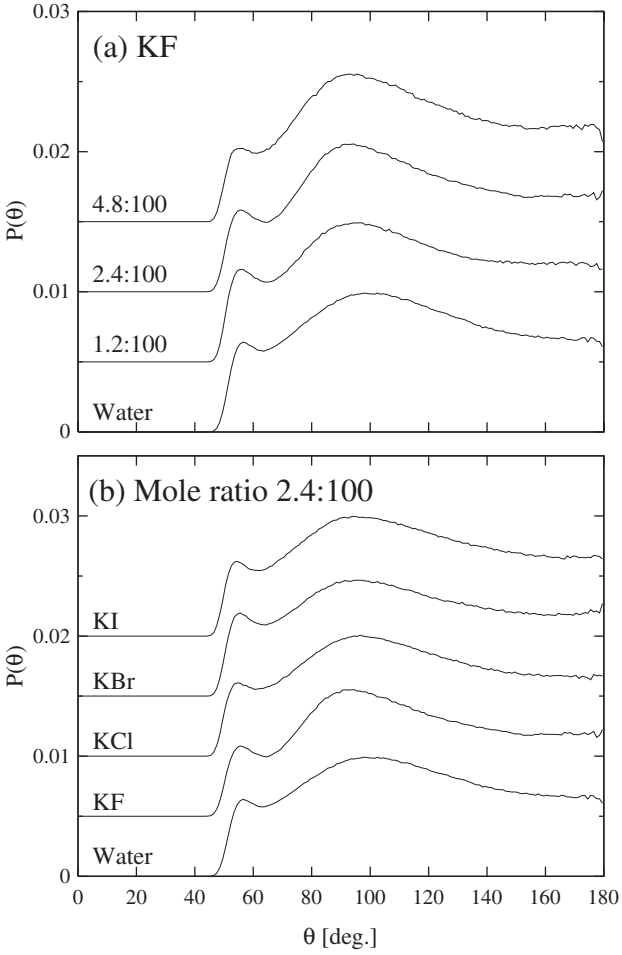

Fig. 10. Ow–Ow–Ow near-neighbour angle distributions for water molecules which are outside the first hydration shell of both anion and cation (as defined in Table 4), as a function of concentration for KF (a) and as a function of halide anion (b) at a mole ratio of 2.4:100. The result for pure water is shown at the bottom of each graph.

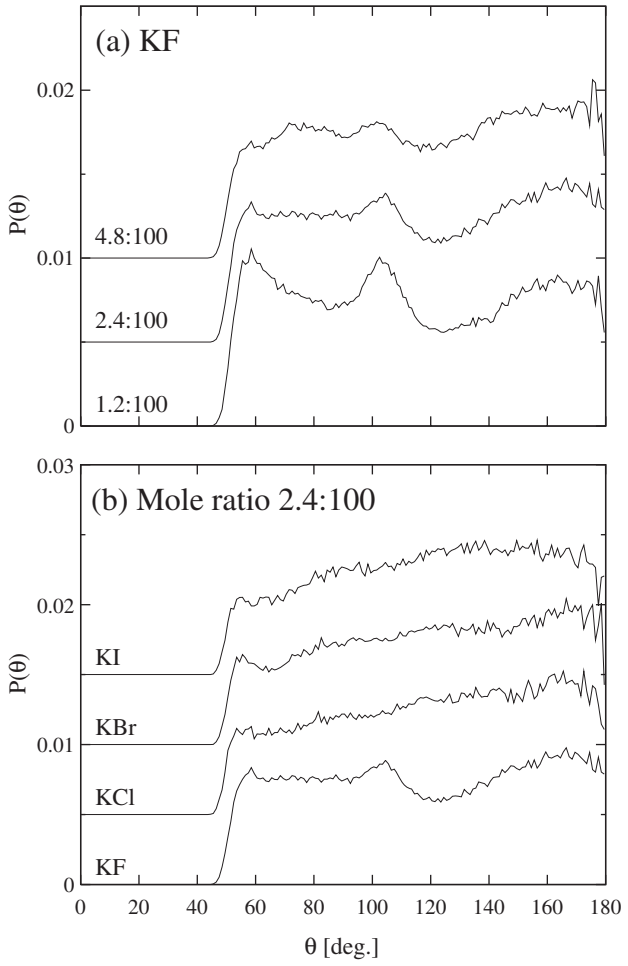

Fig. 11. Ow–Ow–Ow near-neighbour angle distributions for water molecules two of which are inside the first hydration shell of the anion (as defined in Table 4), as a function of concentration for KF (a) and as a function of halide anion (b) at a molar ratio of 2.4:100.

data, then it would be implemented, but so far no satisfactory scheme has been found.

As regards the water structure in these K-halide ionic aqueous solutions, we have seen, Figs. 2 and 3, that overall the structure does not appear to be radically altered in these solutions compared to the bulk liquid, other than some inwards movement of the OwOw second peak with increasing concentration. These graphs do not distinguish between water that is in the first shell of the ions, and water that is outside the first shell. Hence the observed effect with concentration might be a simple consequence of the change of solution composition. To determine whether this is true, we have calculated the Ow–Ow–Ow angle distribution for triplets of water molecule neighbours, none of which are allowed to be in the first hydration shell of either a cation or an anion, as defined by Table 4. Two water molecules are defined as being neighbours if they are 3.3 Å apart or less. The distributions are shown as a function of concentration for KF, Fig. 10(a), and as a function of ion size at a mole ratio of 2.4:100, Fig. 10(b), and in both cases compared to the corresponding angle distribution for bulk water. It is seen that in general the position of the broad peak near 100° for pure water, which is characteristic of the tetrahedral distribution found in water, has moved inwards slightly for all the solutions, but especially in the case of KF at the highest concentration. Hence there is evidence here for some limited, longer range distortion to the water structure when ions are present compared to when they are absent. This therefore is in keeping with the observations that the orientational relaxation time of water away from the ions is unchanged from the bulk liquid [9].

Close to the ions the situation is quite different. To demonstrate this, we calculate the same function, namely the Ow–Ow–Ow angle distribution for triplets of water molecule neighbours, where we require that two of the neighbours must lie within the first shell of a specified ion, and the third can lie anywhere in the solution. In fact the distance constraint between neighbours means that this third molecule will be located either in the first or second shell of the specified ion. Fig. 11(a) shows this restricted angle distribution for the fluoride ion as a function of concentration, whereas Fig. 11(b) shows it for the anion as a function of ion size at a molar ratio of 2.4:100. Fig. 12 shows the same angle distribution for the potassium ion as a function of concentration.

For the larger anions we see that the angular distribution is almost featureless—there is no evidence for the broad peak near

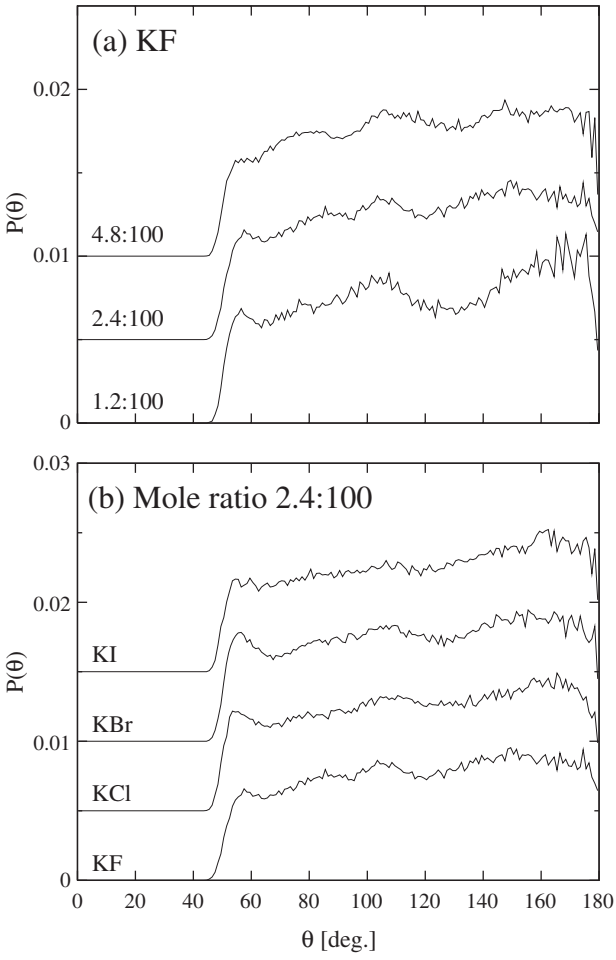

Fig. 12. Ow–Ow–Ow near-neighbour angle distributions for water molecules two of which are inside the first hydration shell of the potassium cation (as defined in Table 4), as a function of concentration for KF (a) and as a function of halide anion (b) at a molar ratio of 2.4:100.

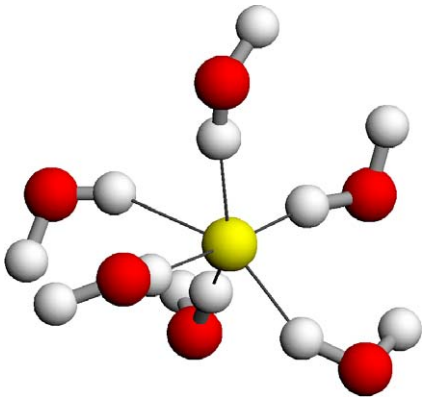

Fig. 13. Example of fluoride ion coordination in mole ratio 1.2:100 KF aqueous solution. The central fluoride ion is shown as yellow, with water oxygen atoms red, and water hydrogen atoms light grey. The water molecule OH vectors are found to be strongly aligned towards the anion.

100° observed for pure water. The hydration shell around these ions is clearly highly disordered compared to bulk water. For fluoride on the other hand there is evidence for something different occurring, especially as the solution becomes more dilute. In particular, in Fig. 11(a) we find a pronounced peak near 60°: this would correspond to water molecules forming a roughly octahedral coordination around the central fluoride ion, Fig. 13, although the distance constraint on neighbouring oxygen atoms being 3.3 Å or less apart, would mean this would have to be significantly distorted. There is also a second well-defined peak near ~103°. This is much sharper than the broad peak near 100° seen in pure water. Since there are no Ow–Ow–Ow angles as large as this if all the oxygen atoms are in an octahedral arrangement in the first shell, this peak can only arise from one of the water molecules being in the second hydration shell, and it indicates that in the immediate vicinity of the fluoride ion, water structure may have indeed been locally enhanced by the ion, although the enhancement is probably offset by distortions at other angles. The effect becomes less obvious at higher concentrations, presumably because there are a greater number of cations in the vicinity of anion, which serve to distort the local arrangement of water more substantially. The same interaction might explain why the water molecules near potassium become more angled in the presence of the fluoride ion, than for the larger anions, Table 5. The water ordering does not appear to happen in the vicinity of the larger anions, and so it would be correct to regard these heavier ions as structure breakers.

Around the potassium, Fig. 12, there is again evidence for the water being highly disordered compared to bulk water—the angle distribution curves show few distinct features, and are almost independent of anion size. There remains therefore the question of whether it makes sense to discuss ions in terms of structure makers and structure breakers. With the possible exception of the fluoride ion, all the ions studied here have a net disordering effect on water structure overall, which is not entirely surprising, given that they significantly orient water molecules away from the tetrahedral bonds they would otherwise adopt in the bulk liquid. Having done this close the ion, the effect on the longer range water structure away from the ions is remarkably weak. This therefore lends weight to the idea that what is important to determining ion properties is the way the ion coordinates water, and not whether it makes or breaks water structure.

6. Conclusion

To summarise the main results of this work: a series of potassium halide aqueous solutions have been investigated as a function of salt concentration and anion size, using neutron diffraction with hydrogen isotope substitution and computer simulation modelling. A general finding is that water is not strongly disordered outside of the hydration shells of the ions. There is some evidence for a mild disordering analogous to what happens to pure water when put under pressure, and this effect seems more marked for the smallest anion and at high concentrations.

In the first hydration shell of the ions, the water appears strongly disordered, with pronounced orientations towards or away from the ion. For the cations the chosen axis is the water molecule dipole moment vector which is on average pointing directly away from the ion, but can be heavily canted at angles up to 80°. For the anions the OH vector is pointing directly at the ion, with an increasing spread of angles as the anion size increases. The exception to the above finding is the fluoride ion at low concentration where the water appears ordered to some extent by the ion in the first shell, by giving a more pronounced tetrahedral peak in the angle distribution (Fig. 11(a)). Beyond this first shell the water appears more like bulk water, although some weak orientational correlations do occur with the all the ions (Fig. 6(b) and Fig. 8(b)).

The ion–ion distributions show definite like–unlike ion contacts above a molar ratio of 1.2:100 (Fig. 9). It was pointed out that for Cl^-, Br^- and I^-, the ion contacts are outside the potassium ion hydration shell, while for F they would be inside. The potassium hydration shell appears slightly more disordered in the fluoride solution than in the other solutions.

It is clear that studies such as these, constrained as they are on local structure information in the form of diffraction data, have the potential to lead to much insight into the structuring of ionic aqueous solutions. There will certainly be ambiguities in the outcome, especially in the more dilute solutions, and for the ion–ion correlations, which are too weakly weighted in the diffraction data to provide useful constraints. What is needed here are better methods of constraining thermodynamic information such as configurational energy and pressure, and better ways of testing alternative hypotheses, such as the idea that fluoride might be tetrahedrally coordinated in the liquid, rather than the octahedral coordination that is found in this work. We hope that progress on these matters will be made in the future.

References

[1] A.V. Okhulkov, Yu. N. Demianets, Yu. E. Gorbaty, J. Chem. Phys. 100 (1994) 1578–1588.
[2] E. Leontidis, Curr. Opin. Colloid Interface Sci. 7 (2002) 81–91.
[3] B. Hribar, N.T. Southall, V. Vlachy, K.A. Dill, J. Am. Chem. Soc. 124 (2002) 12302–12311.

[4] H. Ohtaki, T. Radnai, Chem. Rev. 93 (1993) 1147–1204.
[5] A.K. Soper, J.L. Finney, Phys. Rev. Lett. 71 (1993) 4346–4349.
[6] S. Dixit, A.K. Soper, J.L. Finney, J. Crain, Europhys. Lett. 59 (2002) 377–383;
P. Buchanan, N. Aldiwan, A.K. Soper, J.L. Creek, C.A. Koh, Chem. Phys. Lett. 415 (2005) 89–93.
[7] H.S. Frank, M.W. Evans, J. Chem. Phys. 13 (1945) 507–532.
[8] J. Turner, A.K. Soper, J.L. Finney, Mol. Phys. 77 (1992) 411–429.
[9] A.W. Omta, M.F. Kropman, S. Woutersen, H.J. Bakker, Science 301 (2003) 347–349;
A.W. Omta, M.F. Kropman, S. Woutersen, H.J. Bakker, J. Chem. Phys. 119 (2003) 12457–12461.
[10] J.C. Rasaiah, R.M. Lynden-Bell, Philos. Trans. R. Soc. Lond., A 359 (2001) 1545–1574.
[11] A.K. Soper, Mol. Phys. 99 (2001) 1503–1516.
[12] A.K. Soper, Phys. Rev., B 72 (2005) 104204.
[13] R.D. Mountain, D. Thirumalai, Proc. Natl. Acad. Sci. U. S. A. 95 (1998) 8436–8440.
[14] R.D. Mountain, D. Thirumalai, J. Phys. Chem., B 108 (2004) 19711–19716.
[15] K. Weckstrom, J.B. Rosenholm, J. Chem. Soc., Faraday Trans. 93 (1997) 569–576.
[16] V.F. Sears, Neutron News 3 (1992) 26–37.
[17] A.K. Soper, W.S. Howells, A.C. Hannon, *ATLAS — Analysis of Time-of-flight diffraction data from liquid and amorphous samples.*, Rutherford Appleton Laboratory Report No. RAL-89.046, 1989.
[18] A.K. Soper, A. Luzar, J. Chem. Phys. 97 (1992) 1320–1331.
[19] R.C. Weast (Ed.), Handbook of Chemistry and Physics, 55th edition, CRC Press, Cleveland, 1974.
[20] H.F. Fisher, A.C. Barnes, P.S. Salmon, Rep. Prog. Phys. 69 (2006) 233–299.
[21] R.L. McGreevy, J. Phys., Condens. Matter 13 (2001) R877–R913.
[22] L. Pusztai, Phys. Rev., B 60 (1999) 11851–11854.
[23] G. Hummer, D.M. Soumpasis, M. Neumann, J. Phys., Condens. Matter 6 (1994) A141–A144.
[24] H.J.C. Berendsen, J.R. Grigera, T.P. Straatsma, J. Phys. Chem. 91 (1987) 6269–6271.
[25] S. Chowdhuri, A. Chandra, J. Chem. Phys. 118 (2003) 9719–9725.
[26] R. Leberman, A.K. Soper, Nature 378 (1995) 364–366.
[27] G.J. Herdman, G.W. Neilson, J. Mol. Liq. 46 (1990) 165–179.
[28] S.B. Rempe, D. Asthagiri, L.R. Pratt, Phys. Chem. Chem. Phys. 6 (2004) 1966–1969.
[29] G.W. Neilson, J.E. Enderby, Proc. R. Soc., A 390 (1985) 353–371.
[30] N.T. Skipper, S. Cummings, G.W. Neilson, J.E. Enderby, Nature 321 (1986) 52–53.
[31] F.G. Edwards, J.E. Enderby, R.A. Howe, J. Phys. C. Solid State Phys. 8 (1975) 3483–3490.
[32] F. Bruni, M.A. Ricci, A.K. Soper, in: M. Nardone, M.A. Ricci (Eds.), Francesco Paolo Ricci: His Legacy and Future Perspectives of Neutron Spectroscopy, Italian Physical Society Conference Proceedings, vol. 76, Società Italiana di Fisica, Bologna, Italy, 2001, p. 37.